International Society for Rock Mechanics and Rock Engineering
Norwegian Group for Rock Mechanics

ISRM International Symposium
Eurock 2025 – Expanding the Underground Space
Trondheim, Norway, 16-20 June
ISBN 978-82-8208-079-8

Evaluation of the impact of heating and subsequent liquid nitrogen cooling on the properties of Rajahmundry basalt

Rajeswar Das, Bikash Kumar Ram & Deepak Amban Mishra
Indian Institute of Petroleum and Energy Visakhapatnam, India
raja.rajeswar@iipe.ac.in

Abstract

The influence of temperature on the physico-mechanical properties of rock has drawn considerable attention in recent years in various geotechnical projects such as geothermal energy extraction, underground coal gasification, shale gas production, nuclear waste disposal, enhanced oil recovery, drilling and blasting, and tunnel fires. Basaltic terrain, which is found both in oceanic and continental crust, holds potential for geothermal energy production and underground nuclear waste storage due to its high thermal conductivity, specific heat capacity, hardness, and strength. This study aims to evaluate the effects of heating and cooling on the physical properties and uniaxial compressive strength of basaltic rocks collected from the Rajahmundry Traps, Andhra Pradesh, India. Core samples prepared from these basalt blocks were subjected to thermal treatments at temperatures of 100°C, 200°C, 300°C, 400°C, 500°C, 600°C, and 800°C, followed by rapid cooling using liquid nitrogen (N-C) or slow cooling in atmospheric air (A-C). The study revealed that porosity increased from 1.40% in untreated samples to 3.45% and 4.03% after A-C and N-C treatments at 800°C, respectively. The P-wave velocity (V_P) dropped by ~47% and ~50%, while S-wave velocity (V_S) decreased by ~40% and ~44% after A-C and N-C at 800°C, respectively as compared to untreated specimens. Whereas at the same, the uniaxial compressive strength is observed to be ~-17% and ~-25%, respectively. The observed changes in the physico-mechanical properties of Rajahmundry basalt can be attributed to the evaporation of absorbed water, expansion and contraction of the mineral grains and cracks, or weakening of grain bonding due to the formation of the thermal-induced microcracks.

Keywords

Thermal treatment, LN_2 cooling, Basalt, Ultrasonic velocities, UCS

ISRM

NBG

1 Introduction

With increasing demand for resources relative to their availability, much of the current research focuses on utilizing subsurface resources and the spaces they offer through various underground geotechnical projects like underground exploration of geothermal heat energy, underground disposal of nuclear waste, exploitation of deep mineral resources, underground coal gasification, underground carbon dioxide sequestration, underground tunnelling etc. (Rathnaweera et al. 2018; Ram and Gupta 2024). In all such rock engineering projects, the rock masses are subjected to different degrees of heat, and thus to cool the adjacent insitu rocks or enhance the permeability through hydraulic fracturing, different coolants like water or liquid nitrogen (LN_2) have often been used as a conventional cooling agent or drilling fluid to ease the various drilling operations in routine rock engineering activities. This thermal treatment makes the minerals in rocks, each with distinct melting points, respond differently to thermal effects, leading to thermal expansion, the development of thermally induced cracks as an important factor for governing the physical and mechanical properties of rocks, thereby controlling the safety and sustainability of these structures.

As the real-time test of thermally treated rock is highly expensive and complicated, rocks have been analysed after undergoing thermal treatment in the laboratory. In the recent past, liquid nitrogen (LN_2)-cooling has gained considerable attention as a substitute for conventional water-based cooling techniques and LN_2 has also become common as a potential fracturing agent in the construction of enhanced geothermal system (Kim 2004; Fu-bao et al. 2015; Cai et al. 2014; Wang et al. 2016; Ding et al. 2024). Thus, many researchers have conducted numerous experimental studies to understand the change in the physical and mechanical properties of different rock types like granite, sandstone and limestone etc. due to heating followed by air cooling and LN_2 cooling (Kumari et al. 2017; Wu et al. 2018; Wu et al. 2019b; Xi et al. 2023; Pathiranagei et al. 2021; Ding et al. 2024). From the existing studies, it is evident that the type of thermal treatments or the degree of thermal gradient that induce due to the nature of cooling of heated rocks plays a vital role in controlling the physico-mechanical properties of rocks (Kumari et al. 2017; Ersoy et al. 2017; Pathiranagei et al. 2021; Wu et al. 2019, Ding et al. 2024). Nevertheless, it is also observed that the different rocks with varying mineral content and inherent microstructural characteristics exhibit disparate strength variation pattern with reference to thermal treatments and possess different threshold at which rock properties changes significantly (Tian et al. 2012; Wong et al. 2020; Pathiranagei et al. 2021).

Basalt, a basic volcanic rock abundantly found in both the Earth's oceanic and continental crust, possesses several distinctive properties that make it suitable for various underground geotechnical projects and various building and construction purposes, it has received relatively little attention. Basalt has several properties like moderate to high thermal conductivity, high specific heat capacity, high hardness, and strength (Silva et al. 2021; Zheng et al. 2022). Additionally, basalt possesses low porosity and permeability. Due to its favourable thermal characteristics, basalt serves as an attractive material for sustainable energy solutions. Notably, because of these thermal properties, it is well-suited for geothermal energy storage (Grirate et al. 2016; Becattini et al. 2017). Moreover, its widespread distribution makes it one of the promising terrains for deep geological repositories and nuclear waste disposal sites. However, limited research (e.g. Pathiranagei et al. 2021; Niu et al. 2023; Wang et al. 2024; Qiao et al. 2024) has been conducted to understand how the physico-mechanical properties of basalt evolve after thermal treatment, particularly in relation to heating-LN_2 cooling, for which comprehensive understanding is yet to be achieved.

Accordingly, this study examines the effects of heating and LN_2-cooling on Rajahmundry basalt collected from the Andhra Pradesh region of India. The research investigates changes in effective porosity, ultrasonic velocities like P- wave (V_P) and S- wave (V_S), uniaxial compressive strength (UCS), Young's modulus, and Poisson's ratio across a temperature range of 100°C to 800°C, followed by air and LN_2 cooling, and compares these results with untreated specimens. The findings of this study contribute to understanding thermal damage evolution in basalt at elevated temperatures and support the evaluation of safety and stability in deep rock masses for various underground geoengineering applications confined in basaltic terrain.

2 Methodology

2.1 Sample collection and preparation

Block samples of basalt were collected from Gowripatnam-Pangidi village, located to the west of the Godavari River in Rajahmundry, Andhra Pradesh, India. These basalt exposures are associated with the Rajahmundry Trap Basalts (RTB) in the Krishna-Godavari Basin (Sen et al. 2011). The RTB is primarily comprised of plagioclase (51.5 - 85.3%), along with clinopyroxene (10-40%) and small amounts of titaniferous magnetite and ilmenite (Rao et al. 2012).

From the collected block samples, core samples of NX size (~54.7mm) were drilled using a rock core drilling machine in the laboratory. Subsequently, the drilled core samples were cut by a cutting machine to prepare cylindrical test specimens of dimension L:D = 2:1 for the UCS test, according to ISRM (2009). Both the faces of the prepared cylindrical specimens were polished using a grinding machine to make them smooth and parallel.

2.2 Thermal treatment

The selected specimens are thermally treated under seven different target temperatures (100°C, 200°C, 300°C, 400°C, 500°C, 600°C, and 800°C) to investigate the variation in physico-mechanical properties of basalt. One set of untreated specimens was also analysed for comparative purposes. For thermal treatment, for each target temperature, two sets of specimens were kept in the electric muffle furnace. A slow heating rate of ~10°C/min was employed in this study to reach each target temperature to prevent/minimize the thermal shock in rock during heating (Ersoy et al. 2019; Pathiranagei et al. 2021). After reaching the target temperatures, the same temperature was maintained inside the oven continuously for 2 hours. After this period, the specimens are carefully removed, and one set of samples is placed in a thermostat with LN_2 for rapid cooling treatment before being maintained at room temperature, while the other set is directly kept at room temperature for a slow cooling process. By monitoring the duration required for specimens to return to ambient temperature after being heated to specific target temperatures, the cooling rates for both A-C and N-C methods were determined. The cooling rate is very variable since the samples heated at high temperatures cool down slowly as compared to samples heated at low temperatures. The cooling rate in A-C was estimated to vary between ~2°C/min to ~21°C/min, while in N-C varies between ~2.05°C/min to ~25°C/min for target temperatures from 100°C to 800°C. This infers that the cooling rate was found to be ~19% higher in the case of N-C as compared to A-C at the target temperature of 800°C. It suggests that the higher cooling rates associated with N-C specimens result in a greater thermal gradient, leading to increased thermal damage compared to A-C specimens. On completely cooling to room temperature and acquiring a constant mass, all the specimens were kept in plastic bags until further tests had been performed.

2.3 Measurement of physical and mechanical properties

The physical properties like mass, effective porosity, V_P and V_S were measured before and after the thermal treatment for each specimen to understand the variation in these physical parameters. The dry weight (W_{Dry}), saturated weight (W_{Sat}) and suspended weights (W_{Sus}) of the specimens were measured and the effective porosity values of thermally treated specimens were estimated using the water saturation method by ISRM (2007). The V_P and V_S were measured before and after the thermal treatments using Pundit Lab PROCEQ instruments using two transducers, i.e. V_P (54 kHz) and V_S (40 kHz). The UCS test was performed on thermally treated specimens along with untreated specimens using a servo-controlled GCTS RTR-3000 universal testing machine. The axial and circumferential deformation values were also measured during the UCS test using two axial and one lateral linear variable differential transducer (LVDTs) with an accuracy of 0.001mm. All the tests have been done with axial strain control with a strain rate of 0.05% per minute. The peak strength of each specimen was recorded and elastic parameters like Young's modulus and Poisson's ratio have been calculated from the linear region of each stress-strain plot.

3 Results

The variation in effective porosity under different thermal treatments is shown in Fig. 1 a). From Fig. 1(a) it is observed that there is no significant change in effective porosity up to 500°C, with a slight decrease. At 500°C, the effective porosity of the basalt specimen is decreased to ~0.7% and 1% for A-

C and N-C samples, respectively. Beyond this temperature the effective porosity significantly increased up to 800°C. At 800°C, the effective porosity rises to ~3.45% and ~4.035, which is increased by ~146% and ~187% in the case of A-C and N-C samples, respectively, compared to untreated specimens.

The V_P and V_S values for thermally treated basalts were measured before and after the thermal treatment and the rate of change in V_P ($K(V_P)$) and V_S ($K(V_S)$) for different thermal treatments was calculated using Eq. 1.

$$K(V_X) = \frac{(V_X)_T - (V_X)_O}{(V_X)_O} \times 100(\%) \quad (1)$$

Where $(V_X)_T$ V_P /V_S before thermal treatments

$(V_X)_O$ V_P /V_S after the thermal treatments

The result of the rate of change in V_P and V_s are presented in Fig. 1b and c. It is evident that both the ultrasonic velocities change at a slower rate up to thermal treatments of 200°C. However, beyond this temperature, the thermal treatments cause a drop in velocities with a higher drop in case N-C specimens as compared to A-C specimens. The rate of change of V_P and V_S is found to be ~-47% and ~-40%, respectively, for A-C specimens and ~-50% and ~-44% respectively, for N-C specimens after thermal treatment at 800°C with reference to thermally untreated specimens (Fig. 1b and c).

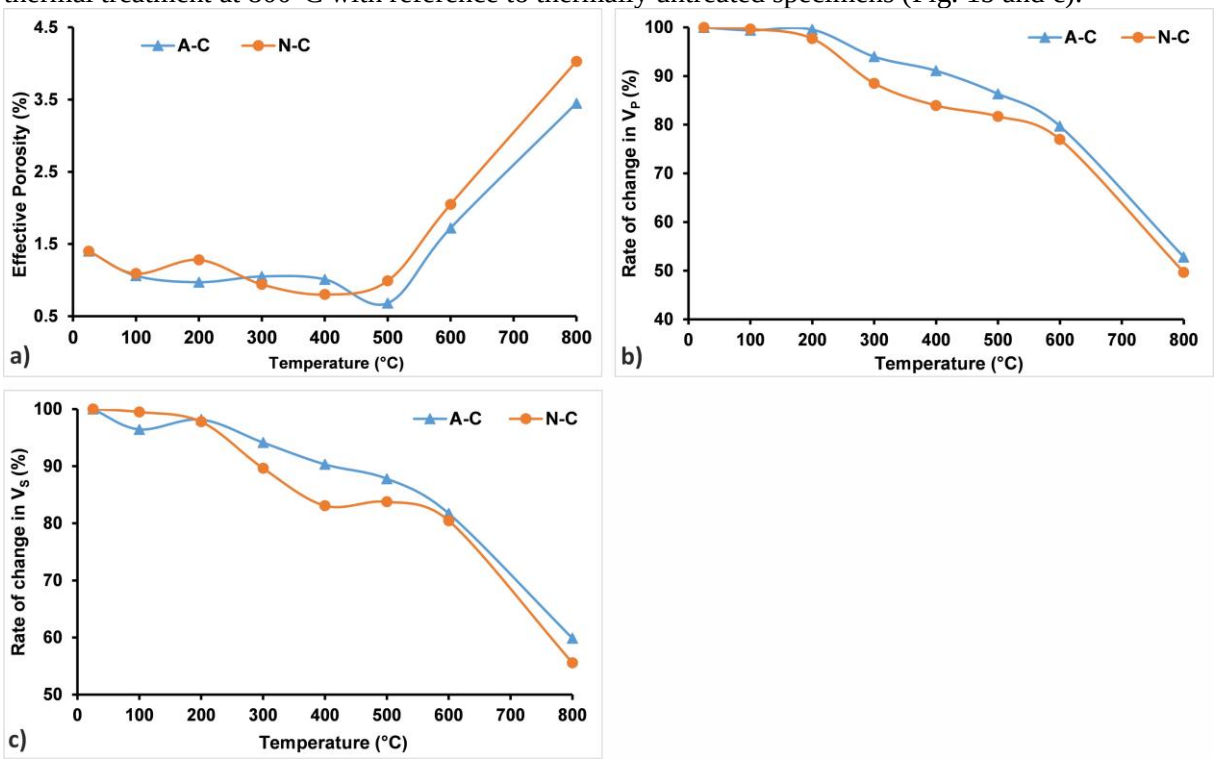

Fig. 1a) Change in effective porosity; b) Rate of change of V_P and c) Rate of change of V_S due to thermal treatments

The variation in UCS at different thermal treatments is shown in Fig. 2(a). From the figure, it is observed that no significant change in peak strength was observed up to 300°C in the case of A-C specimens. However, with further increase in temperature of thermal treatment results in an increase of UCS, which is estimated to be ~15% at 500°C with reference to untreated specimen. With further increase in temperature, the UCS gradually decreases and becomes ~-17% at 800°C compared to the untreated specimens (Fig. 2a). Whereas, in the case of LN_2-cooled specimens, UCS initially has minimal variation at 100°C, followed by a decrease of ~8% at 200°C (Fig. 2a). A further increase in the temperature of thermal treatment results in an increase in UCS up to 500°C, which further decreases at higher temperatures and has been estimated to be ~-25% at 800°C compared to untreated specimens. Similarly, with increased temperature of thermal treatment, the variation in Young's modulus also shows a similar variation to the variation in UCS shown in Fig. 2(b). From the Fig. 2(b) it is observed that there is minimal variation in Young's modulus up to 400°C for both A-C and N-C specimens. However, with further increases in temperature, Young's modulus initially increased by approximately ~12% and ~6% at 500°C. Beyond this temperature, it decreased significantly, dropping by around ~56% and ~63% at 800°C for the A-C and N-C specimens, respectively, compared to untreated specimens (Fig. 2b). The variation in Poisson's ratio with temperature, as shown in Fig. 2 c, exhibits minimal change up to 300°C compared to untreated specimens. However, with further

increases in the temperature of thermal treatments, this variation becomes more pronounced, increasing by ~76% and ~91% at 800°C for the A-C and N-C specimens, respectively, relative to untreated specimens. Fig. 3 presents the representative response of the stress-strain response of basalt specimens after undergoing different thermal treatments. As shown in Fig. 3, the stress-strain relationships of basalt specimens vary significantly beyond 500°C. Beyond this temperature, the nonlinearity in the deformation stage of the axial stress-strain curve gradually becomes more pronounced.

4 Discussion

Under normal conditions, Rajahmundry basalts exhibit a low effective porosity of ~1.4%. It is observed that the effective porosity decreases up to 500°C in both thermal treatments. This could be attributed to the mineral grain expansion and dehydration of structural water, resulting in a more compact structure. The thermal treatments at higher temperatures > 500°C cause a rapid increase in effective porosity with a higher increase in the case of N-C specimens, likely due to the formation of additional thermally induced microcracks caused by greater thermal gradients. The rate of change in V_P and V_S indicates a gradual decrease as temperature increases for both the cooling methods (Fig. 1b & c) with a higher reduction in N-C specimens, indicating greater microstructural damage inside the specimens because of the quenching effect due to higher thermal gradient and sudden cooling. To substantiate the internal damage in the rock, the damage factor (D(P)) was calculated using measured V_P values and the following Eq. 2. (Liu et al. 2015; Yang et al. 2019)

$$D(P) = 1 - \left(\frac{V_T}{V_O}\right)^2 \tag{2}$$

Where $D(P)$ the damage factor
V_O the initial V_P
V_T the V_P after the thermal treatment

As shown in Fig. 2 (d), the damage factor increases progressively with rising temperature, and it also shows that LN_2-cooled specimens exhibit a higher damage factor compared to A-C specimens beyond 300°C. Consequent to the thermal treatment-induced physical changes, the mechanical properties also vary with different thermal treatments. Since the thermal expansion of mineral grains and dehydration of structural water led to a denser, more compact structure to the basaltic specimens up to 500°C, it resulted in higher UCS and Young modulus values and lower Poisson's ratio values.

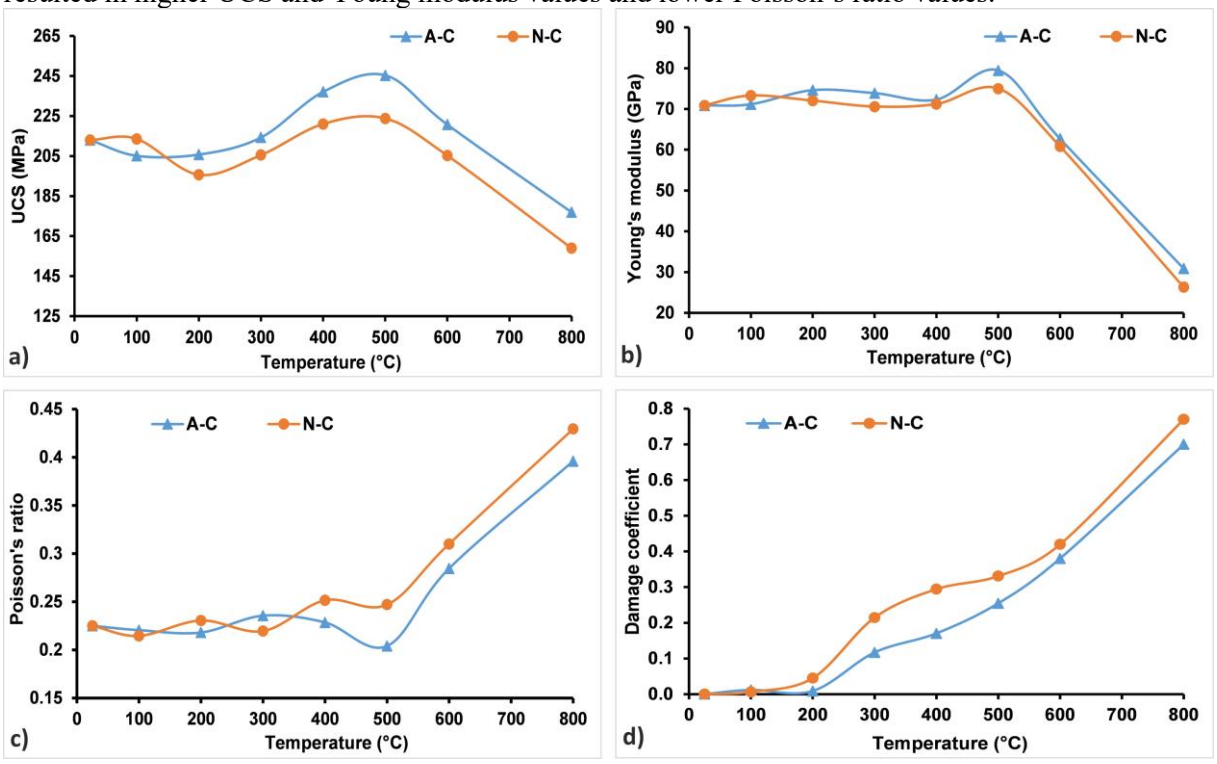

Fig. 2(a) Variation in UCS (b) Young's modulus (c) Poisson's ratio and (d) damage coefficient after different thermal treatments

In this study, the inflection point was found at 500°C, beyond which there is a substantial increase in effective porosity and a decrease in UCS, elastic modulus. Conversely, at temperatures below 500°C, there is, no significant change in effective porosity, UCS, or elastic modulus is observed. However, the same is not evident in the case of ultrasonic velocities after thermal treatment. Rather, it shows a gradually decreasing trend from 100°C to 800°C. This could be attributed to the nature of wave propagation, which not only depends on crack development but also on various microstructural variables such as mineralogy and the shape, size, density, and orientation of pores and grains (Basu and Aydin, 2005). An increase in temperature leads to greater internal damage within the rock, manifested as the formation of additional thermally induced microcracks and their coalescence with pre-existing microcracks (Collin and Rowcliffe 2002; Fellner and Supanic 2002; Tian et al. 2012; Ram and Gupta 2024). This damage is more pronounced in N-C specimens, resulting in a greater reduction in mechanical properties at higher temperatures compared to A-C specimens. Similar observation of deterioration of mechanical properties of basalt at higher temperature >500°C is also obtained by Pathiranagei et al. 2021, Niu et al. 2023, Wang et al. 2024, Qiao et al. 2024.

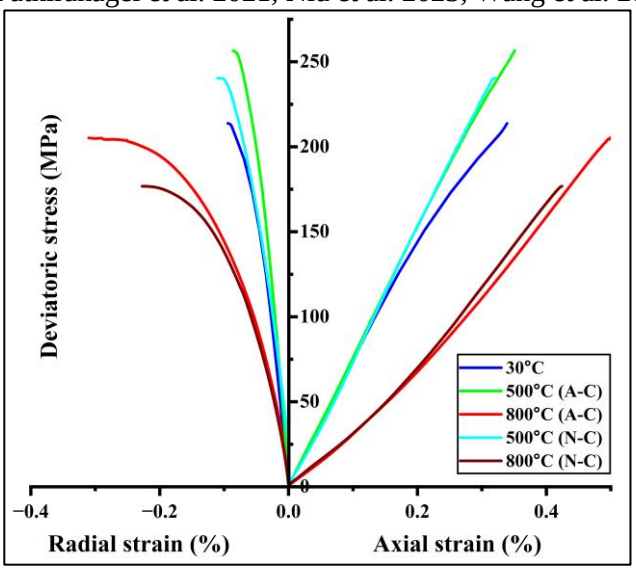

Fig. 3 Stress-strain curve of basalt specimens after different thermal treatments (A-C: air cooling; N-C: LN_2 cooling)

5 Conclusion

The conclusions of this study can be outlined as follows:

- The initial increase in temperature leads to the expansion of mineral grains and dehydration of structural water, causing the basalt to develop a more compact structure, which reduces its effective porosity up to 500°C. However, at thermal treatments >500°C, it causes the generation and coalescence of additional thermally induced microcracks, which results in an increase in porosity with higher values in N-C specimens as compared to A-C specimens. This could be attributed to the quenching effect in the former that induces a higher thermal gradient, leading to more damage in the rock.
- The different thermal treatment-induced microstructural damage could be well substantiated by the drop in ultrasonic wave velocities and damage coefficients, which infers greater damage in N-C specimens as compared to A-C specimens.
- Consequent to the thermally induced physical changes, the UCS and Youngs modulus are found to be ~245 MPa and 79 GPa at 500°C and ~177 MPa and ~31 GPa at 800°C in the case of A-C specimens and ~224 MPa and ~75 GPa at 500°C and ~159 MPa and ~26 GPa at 800°C in case of N-C specimens.
- Similarly, after thermal treatment, the Poisson's ratio value was found to be 0.4 and 0.43 at 800°C in the case of A-C and N-C specimens, respectively, relative to 0.23 for untreated specimens.

The microstructural studies through investigating the rock specimens under micro-CT and observing the thin sections under the petrological microscope will be further employed in future to better substantiate the present work and comprehend a better understanding of the effects of different thermal treatments on physico-mechanical properties of basalt.

Acknowledgement

The author thanks the Indian Institute of Petroleum & Energy, Visakhapatnam, India, for providing the overall support to carry out this research work. The first author also acknowledges the Indian Institute of Petroleum & Energy and MoPNG for the PhD research fellowship. The second author also acknowledges DST-SERB for the NPDF fellowship (Grant id: PDF/2022/002111)

References

Basu, A., & Aydin, A. (2006). Evaluation of ultrasonic testing in rock material characterization. *Geotechnical Testing Journal*, *29*(2), 117-125.https://doi.org/10.1520/GTJ12652

Becattini, V., Motmans, T., Zappone, A., Madonna, C., Haselbacher, A., & Steinfeld, A. (2017). Experimental investigation of the thermal and mechanical stability of rocks for high-temperature thermal-energy storage. Applied Energy (203): 373-389. https://doi.org/10.1016/j.apenergy.2017.06.025

Cai, C., Li, G., Huang, Z., Shen, Z., Tian, S., & Wei, J. (2014). Experimental study of the effect of liquid nitrogen cooling on rock pore structure. Journal of Natural Gas Science and Engineering (21): 507-517. https://doi.org/10.1016/j.jngse.2014.08.026

Collin, M., & Rowcliffe, D. (2002). The morphology of thermal cracks in brittle materials. Journal of the European Ceramic Society 22(4): 435-445. https://doi.org/10.1016/S0955-2219(01)00319-3

da Silva, B. A., Calegari, M. R., Pinheiro, M. R., & Fujita, R. H. (2021). Lithostructural and tectonic determinants in the geomorphic evolution of the Basalt Plateau–Southern Brazil. Journal of South American Earth Sciences (110): 103351. https://doi.org/10.1016/j.jsames.2021.103351

Ding, R., Sun, Q., Jia, H., Tang, L., & Li, D. (2024). Experimental Study on the Compressive Strength and AE Characteristics of High-Temperature–Treated and LN2-Cooled Sandstone. *International Journal of Geomechanics*, *24*(4), 04024040. https://doi.org/10.1061/IJGNAI.GMENG-9010

Ersoy, H., Kolaylı, H., Karahan, M., Harputlu Karahan, H., & Sünnetci, M. O. (2019). Effect of thermal damage on mineralogical and strength properties of basic volcanic rocks exposed to high temperatures. Bulletin of Engineering Geology and the Environment (78): 1515-1525. https://doi.org/10.1007/s10064-017-1208-z

Fellner, M., & Supancic, P. (2002). Thermal shock failure of brittle materials. Key Engineering Materials (223): 97-106. https://doi.org/10.4028/www.scientific.net/KEM.223.97

Fu-bao, Z., Bo-bo, S., Jian-wei, C., & Ling-jun, M. (2015). A new approach to control a serious mine fire with using liquid nitrogen as extinguishing media. *Fire Technology*, *51*, 325-334. https://doi.org/10.1007/s10694-013-0351-8

Grirate, H., Agalit, H., Zari, N., Elmchaouri, A., Molina, S., & Couturier, R. (2016). Experimental and numerical investigation of potential filler materials for thermal oil thermocline storage. Solar energy (131): 260-274. https://doi.org/10.1016/j.solener.2016.02.035

Hatheway, A. W. (2009). The complete ISRM suggested methods for rock characterization, testing and monitoring; 1974–2006. https://doi.org/10.2113/gseegeosci.15.1.47

ISRM, the complete ISRM suggested methods for rock characterization, testing and monitoring: 1974–2006. In: Ulusay R, Hudson JA (eds) Suggested methods prepared by the commission of testing methods, ISRM, compilation arranged by the ISRM Turkish national group, Kozan Ofset, Ankara (2007).

Kumari, W. G. P., Ranjith, P. G., Perera, M. S. A., Chen, B. K., & Abdulagatov, I. M. (2017). Temperature-dependent mechanical behaviour of Australian Strathbogie granite with different cooling treatments. *Engineering Geology*, *229*, 31-44.Kim, A. G. (2004). Cryogenic injection to control a coal waste bank fire. *International Journal of Coal Geology*, *59*(1-2), 63-73. https://doi.org/10.1016/j.enggeo.2017.09.012

Liu, S., & Xu, J. (2015). An experimental study on the physico-mechanical properties of two post-high-temperature rocks. Engineering Geology (185): 63-70. https://doi.org/10.1016/j.enggeo.2014.11.013

Nageswara Rao, P. V., Swaroop, P. C., & Karimulla, S. (2012). Mineral chemistry of Pangidi basalt flows from Andhra Pradesh. Journal of Earth System Science (121): 525-536. https://doi.org/10.1007/s12040-012-0174-x

Niu, Y., Wang, G., Wang, J., Liu, X., Zhang, R., Qiao, J., & Zhang, J. (2023). Experimental study on thermal fatigue damage and failure mechanisms of basalt exposed to high-temperature treatments. *Fatigue & Fracture of Engineering Materials & Structures*, *46*(8), 2909-2928. https://doi.org/10.1111/ffe.14052

Qiao, J., Wang, G., Song, L., Liu, X., Zhou, C., Niu, Y., & Liu, B. (2024). Mechanical properties and the mechanism of microscopic thermal damage of basalt subjected to high-temperature treatment. *Natural Hazards*, *120*(1), 41-61. https://doi.org/10.1007/s11069-023-06191-8

Ram, B. K., & Gupta, V. (2024). Physico-mechanical characterization of Higher Himalayan granite under the thermal treatments of different heating–cooling conditions. Acta Geotechnica :1-14. https://doi.org/10.1007/s11440-023-02224-5

Rathnaweera, T. D., Ranjith, P. G., Gu, X., Perera, M. S. A., Kumari, W. G. P., Wanniarachchi, W. A. M., ... & Li, J. C. (2018). Experimental investigation of thermomechanical behaviour of clay-rich sandstone at extreme temperatures followed by cooling treatments. International Journal of Rock Mechanics and Mining Sciences (107): 208-223. https://doi.org/10.1016/j.ijrmms.2018.04.048

Sen, B., & Sabale, A. B. (2011). Flow-types and lava emplacement history of Rajahmundry Traps, west of River Godavari, Andhra Pradesh. Journal of the Geological Society of India (78): 457-467. https://doi.org/10.1007/s12594-011-0111-7

Tian, H., Kempka, T., Xu, N. X., & Ziegler, M. (2012). Physical properties of sandstones after high temperature treatment. *Rock mechanics and rock engineering*, *45*, 1113-1117. https://doi.org/10.1007/s00603-012-0228-z

Vidana Pathiranagei, S., Gratchev, I., & Kong, R. (2021). Engineering properties of four different rocks after heat treatment. Geomechanics and Geophysics for Geo-Energy and Geo-Resources (7): 1-21. https://doi.org/10.1007/s40948-020-00211-8

Wang, G., Song, L., Liu, X., Ma, X., Qiao, J., Chen, H., & Wu, L. (2024). Mechanical properties and damage evolution characteristics of thermal damage basalt under triaxial loading. *Rock Mechanics and Rock Engineering*, *57*(2), 1117-1135. https://doi.org/10.1007/s00603-023-03613-8

Wang, P., Xu, J., Liu, S., & Wang, H. (2016). Dynamic mechanical properties and deterioration of red-sandstone subjected to repeated thermal shocks. *Engineering Geology*, *212*, 44-52. https://doi.org/10.1016/j.enggeo.2016.07.015

Wong, L. N. Y., Zhang, Y., & Wu, Z. (2020). Rock strengthening or weakening upon heating in the mild temperature range?. *Engineering Geology*, *272*, 105619. https://doi.org/10.1016/j.enggeo.2020.105619

Wu, X., Huang, Z., Li, R., Zhang, S., Wen, H., Huang, P., ... & Zhang, C. (2018). Investigation on the damage of high-temperature shale subjected to liquid nitrogen cooling. Journal of Natural Gas Science and Engineering (57): 284-294. https://doi.org/10.1016/j.jngse.2018.07.005

Wu, X., Huang, Z., Song, H., Zhang, S., Cheng, Z., Li, R., ... & Dai, X. (2019). Variations of physical and mechanical properties of heated granite after rapid cooling with liquid nitrogen. *Rock Mechanics and Rock Engineering*, *52*, 2123-2139. https://doi.org/10.1007/s00603-018-1727-3

Xi, Y., Wang, H., Jiang, J., Fan, L., Li, J., & Guo, B. (2023). Impacts of different cooling methods on the dynamic tensile properties of thermal-treated granite. *International Journal of Rock Mechanics and Mining Sciences*, *169*, 105438. https://doi.org/10.1016/j.ijrmms.2023.105438

Yang, J., Fu, L. Y., Zhang, W., & Wang, Z. (2019). Mechanical property and thermal damage factor of limestone at high temperature. International Journal of Rock Mechanics and Mining Sciences (117): 11-19. https://doi.org/10.1016/j.ijrmms.2019.03.012

Zheng, Y., Zhuo, J., Zhang, P., & Ma, M. (2022). Mechanical properties and meso-microscopic mechanism of basalt fiber-reinforced recycled aggregate concrete. Journal of Cleaner Production (370): 133555. https://doi.org/10.1016/j.jclepro.2022.133555